Atmósfera (1997), **10**, *pp. 1-22*

Impact of different radiation transfer parameterization schemes in a GCM on the simulation of the onset phase of Indian summer monsoon

JOHN P. GEORGE and Z. N. BEGUM

National Centre for Medium Range Weather Forecasting, Department of Science and Technology, Mausam Bhavan Complex, Lodi Road, New Delhi-110003, INDIA

(Manuscript received January 23, 1996; accepted in final form June 29, 1996)

RESUMEN

Se presenta en este trabajo el impacto de dos esquemas de parametrización de radiación (NASA/Goddard y GFDL) en el modelo T80 del NCMRWF (Centro Nacional de Pronóstico del Tiempo a Mediano Plazo) en la simulación de junio de 1995. Nuestra mira principal aquí es entender la sensibilidad de equemas radiacionales diferentes en la simulación de la fase inicial del monzón veraniego índico.

En la superficie de la Tierra, usando para la simulación el esquema NASA/Goddard se obtiene un equilibrio más razonable entre los flujos entrantes y salientes (flujos térmicos radiativos y turbulentos), que el esquema GFDL. La inclusión de la dispersión por nubes y, por lo tanto, el tratamiento separado de la radiación difusa y la directa en el esquema radiativo NASA/Goddard produjo cambios en el flujo neto de onda corta en la superficie y consiguientemente, en la temperatura superficial. Los resultados indican también la alta sensibilidad por temperatura en superficie, en la simulación del inicio del monzón. Ambos modelos simulan razonablemente los patrones de flujo promedios de junio de 1995.

La comparación entre las dos simulaciones muestra que el modelo T80 con NASA/Goddard tiene menos errores de pronóstico a 200 hPa, en tanto que a 850 hPa esta simulación muestra errores de pronóstico ligeramente mayores al este de los 75°E de longitud en las latitudes de la India.

ABSTRACT

The impact of two radiation parameterization schemes (NASA/Goddard and GFDL) in NCMRWF T80 model on the simulation of June, 1995 is presented in this paper. Our main aim here is to understand the sensitivity of different radiation schemes on the simulation of Indian summer monsoon onset phase. At Earth's surface, the simulation using NASA/Goddard scheme produces more reasonable balance between incoming and outgoing fluxes (radiative and the turbulent heat fluxes) compared to GFDL scheme. The inclusion of cloud scattering and hence the treatment of direct and diffused radiation separately in NASA/Goddard radiation scheme resulted in changes in the net shortwave flux at surface and hence in the surface temperature. Results also indicate the high sensitivity of surface temperature in the monsoon onset simulation. Both models reasonably simulate the mean June 1995 flow patterns. Comparison between the two simulations shows that T80 model with NASA/Goddard has less forecast errors at 200 hPa, whereas in 850 hPa this simulation has slightly higher forecast errors east of 75°E longitude over Indian latitudes.

1. Introduction

Small changes in the radiative energy available at the surface as well as in the atmosphere has a strong impact on the climate scale integrations of general circulation models. However, its role in the medium-range and extented range integrations are yet to be established. Slingo *et al.* (1988) discussed the importance of the physical parameterization, mainly convection and radiation, on the prediction of 1979 summer monsoon onset. Morcrette (1990) had conducted a detailed study on the performance of two different radiation schemes on long-range prediction in the ECMWF model on tropical as well as extratropical regions. But the detailed understanding of the impact of changes in the radiative energy gain/loss of the atmosphere and the Earth's surface on Indian summer monsoon circulation is not clearly established so far. However, this may have an important role in the simulation of the Indian summer monsoon. At the National Centre for Medium Range Weather Forecasting (NCMRWF, India), we have made an attempt to assess the impact of two different radiation schemes, GFDL radiation scheme (Campana *et al.*, 1988; Fels and Schwarzkopf, 1975; Schwarzkopf and Fels, 1991; Lacis and Hansen, 1974) and NASA/Goddard radiation scheme (Harshvardhan *et al.*, 1987) in the T80 model on the simulation of onset phase of Indian summer monsoon.

2. Methodology

A hybrid (emissivity plus band model approach) scheme is used for longwave computations in the GFDL radiation parameterization scheme. In the NASA/Goddard scheme, a broadband parameterization technique is used for the longwave computation. All clouds except high clouds are treated as black bodies in GFDL longwave scheme. But in NASA/Goddard longwave scheme, temperature-dependent emissivity is assumed for all types of clouds.

For clear sky shortwave (SW) computation, the GFDL scheme mainly follows the approach of Lacis and Hansen, 1974. NASA/Goddard scheme also follows the same approach as that of GFDL scheme except in the case of CO_2 absorption and water vapor absorption below 0.9 μm wavelength, which is not included in NASA/Goddard scheme. For the cloudy sky computation, fixed absorption and reflection is considered for all low, medium and high clouds in GFDL scheme, whereas in the NASA/Goddard scheme, two stream approximations with delta-Eddigton technique is used. Main features of the two radiation schemes are presented in Table 1. In both experiments, Slingo (1987) type clouds are used. All other physical processes are identical in both the models.

The following sections describe the comparison of a thirty day integration of the NCMRWF T80 model with NASA/Goddard radiation scheme (NG) and the NCMRWF T80 model with GFDL radiation scheme (GF). Since the aim of this paper is to understand more about the long term impact of different radiation schemes in the NCMRWF T80 model on the simulation of the onset phase of monsoon circulation, the initial condition is choosen as 1st June 1995. With one pair of runs, statistically significant performance assessment of forecast may not be possible. But in this study we have only tried to find out the impact of different radiation parameterization schemes on the onset phase 'climate' of NCMRWF T80 model. So we have tried for comparison of some of the simulated fields with observations, which may provide useful information about the behaviour of NG and GF. Also, we have computed the forecast errors (forecast- verifying NCMRWF analysis) of both the model forecasts for all the thirty days of integration. Both models are forced, throughout the 30-day integration, with climatological sea surface temperature.

TABLE 1

Summary of the GFDL & NASA/Goddard radiation code

	GFDL	NASA/Goddard
a. CLEAR SKY		
(i) Shortwave		
Rayleigh scattering	Included	Included
Aerosol scattering and absorption	Not included	Not included
H_2O	k-distribution method (9 sub intervals over entire SW)	k-distribution method (5 sub intervals over IR only)
CO_2	Overlap with H_2O in IR region	Not included
O_3	Overlap with H_2O in visible & UV	Two bands (in visible & UV)
(ii) Longwave		
H_2O	6 bands for emissivity method and 14 band for random band model	Two band centers and four band wings
CO_2	Two bands (overlap with H_2O)	One band center & two band wings (overlap with H_2O)
O_3	One band (overlap with H_2O)	One band (overlap with H_2O)
Aerosol	Not included	Not included
b. CLOUDY SKY		
(i) Shortwave		
Cloud	Fixed reflectivity and absorptivity	Delta-Eddington method (preset scattering optical depth and asymmetry factor)
(ii) Longwave		
Cloud	Fixed emissivity	Temperature dependent emissivity

3. Results and Discussion

This section has three parts. The first part describes the global energy budgets. The second part deals with the radiative and turbulent heat fluxes over the Indian region produced by the models. The third part discusses the circulation features of Indian summer monsoon by both models.

3.1 Global budgets

The global energy budgets for the atmosphere, surface and the hydrological cycles are affected by the changes in the radiation parameterization. Since in both models the astronomical computations are identical, the incoming solar radiation at the top (solar constant) is equal, with the global mean value of 332 W/m^2 for June. Figure 1 shows that, in both models, the shortwave energy absorbed by the atmosphere is not much different even though GF shows slightly more absorption.

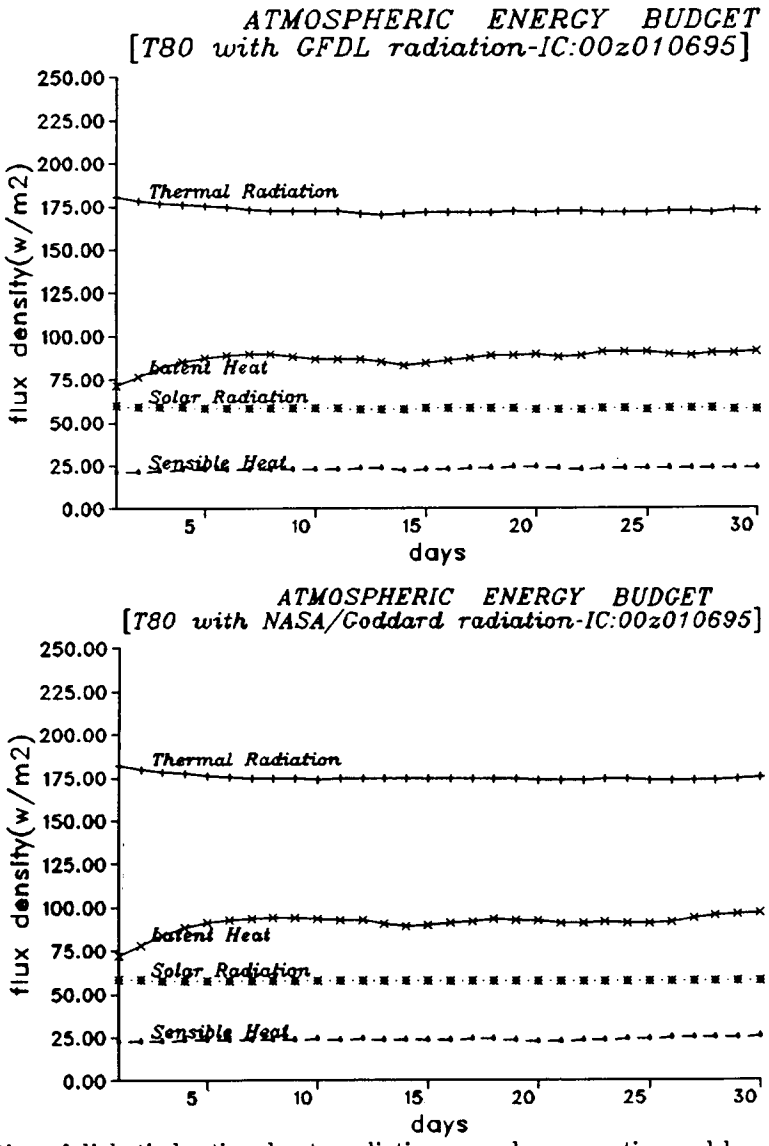

Fig. 1. Time evolution of diabatic heating due to radiation, cumulus convection and large-scale condensation and turbulent heat transfer for the whole globe in the 30 day integration based on the 01 June 1995, 00Z initial condition by NCMRWF T80 model with GFDL (top) and NASA/Goddard (bottom) radiation schemes.

The surface energy budget of both models is displayed in Figure 2. One significant difference is seen in the shortwave radiation absorbed at the surface. NG shows a significantly higher surface absorption as compared to GF. In GF, the 1995 June average value is 171.8 W/m^2 whereas in NG it is 187.2 W/m^2 (Fig. 3). Due to this, both latent heat and sensible heat fluxes are larger in NG than in GF. The total turbulent heat fluxes from the surface is 110.3 W/m^2 in GF whereas in NG it is 114.9 W/m^2, which is closer to the climatology. In both models, the global average cloudiness is around 10% less when compared to climatological data. This is reflected in the higher outgoing longwave radiation (OLR) values, which is higher than the satellite annual mean climatology (Ramanathan, 1987). At the surface, NG shows a more reasonable balance in the incoming and outgoing fluxes as compared to GF, even though Figure 3 results are computed using a one month integration with which it is difficult to conclude the quality of the fluxes produced by the models.

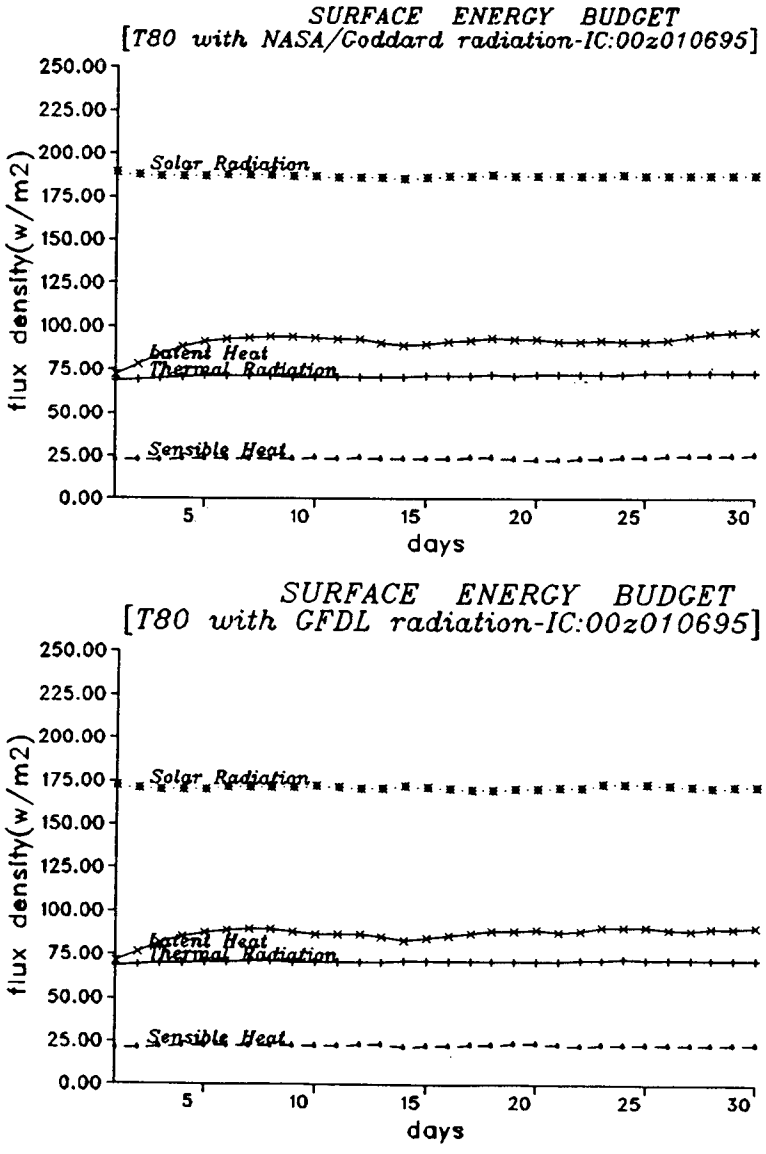

Fig. 2. As in Fig. 1 but for the components of the surface energy budget.

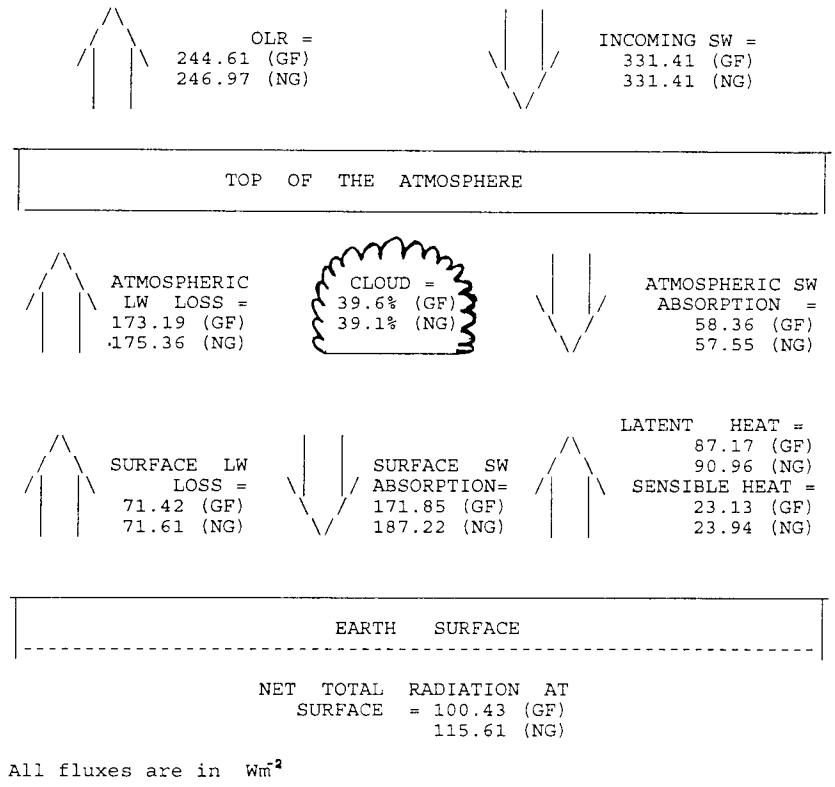

Fig. 3. Mean June 1995 surface and atmospheric energy budget in the 30 day integration based on 00z 01-06-1995 by NG and GF

The changes in the surface energy balance are reflected in higher values (+.5°K) of global mean land surface temperature (Fig. 4). But in both models, the surface temperature trends are similar. Due to the higher values of the surface temperature, higher latent and sensible heat

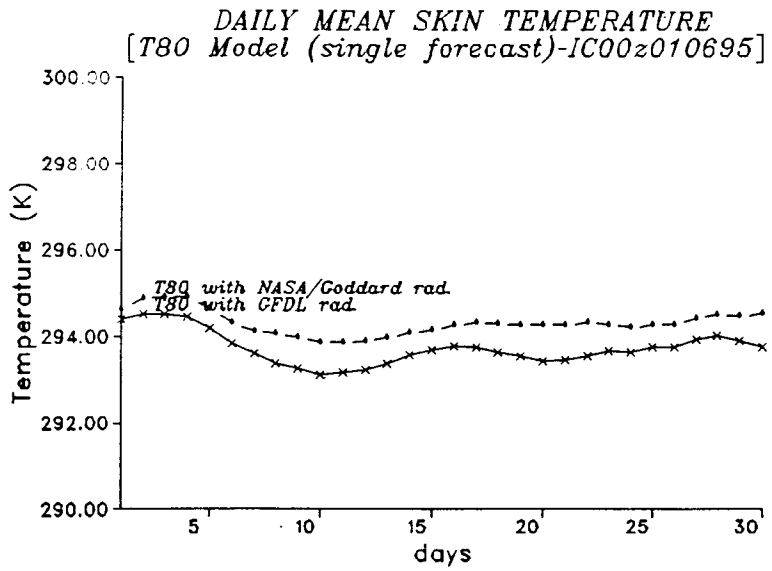

Fig. 4. Time evolution of global mean land surface temperature in the 30 day integration based on 00z 01-06-1995 by NG and GF.

fluxes are seen in NG. It is noted that there is a slight increase in the net surface longwave flux in NG than GF. This increase is in phase with the increase of surface temperature. The higher values of evaporation over land is reflected in the increase in the global average rainfall (Fig. 5). GF and NG indicate the same trends in the total global average precipitation. But in both, the evaporation exceeds precipitation on the fifth day. Thereafter, except for a few days, evaporation rates are more compared to precipitation rates. Another interesting feature noted is the significantly higher precipitation over land in the NG. This is mainly due to the higher land surface temperature and hence the higher evaporation rates.

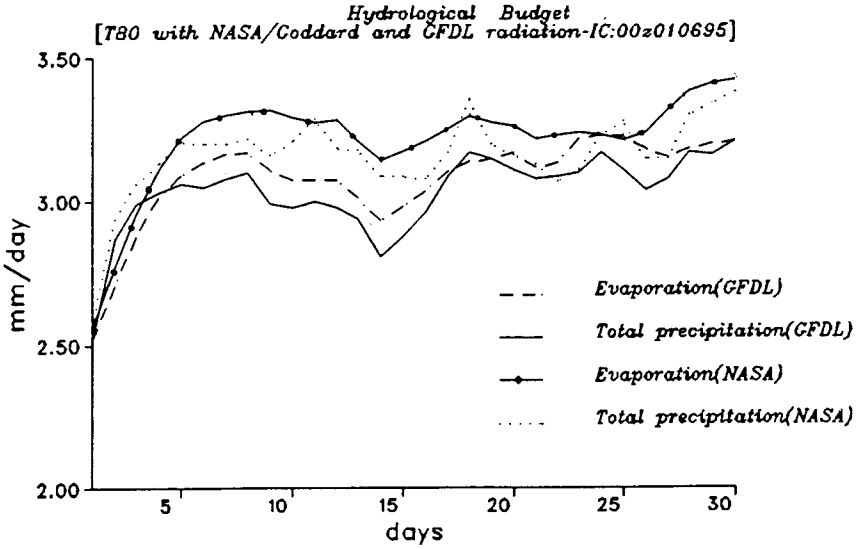

Fig. 5. As in Fig. 1, but for total precipitation and surface evaporation.

3.2 Radiative fluxes over Indian region

3.2.1 Shortwave fluxes over Monsoon region

Net shortwave radiation absorbed by the Earth-Atmospheric System (Fig. 6) shows higher values in NG than in GF over most of land regions except in a few pockets. In these regions, the cloud amounts are also higher in NG (Fig. 7). But over most of the regions the differences are less than 20 W/m^2. Higher values of the shortwave energy absorbed by Earth-Atmospheric System in the NG is mostly due to the higher surface absorption over the land regions.

The changes in the shortwave absorption due to atmospheric gases and clouds in the NG and GF are small, but NG shows slightly lesser atmospheric shortwave absorption over most of the regions (Fig. 8). This may be partly due to the difference in treatment of CO_2 and water vapor below 0.9 μm wavelength in NASA/Goddard and GFDL radiation schemes. In the GFDL shortwave scheme, CO_2 absorption and water vapor absorption below 0.9 μm are included in spite of the fact that they are weak. In the NASA/Goddard scheme, however these weak absorptions are not incorporated. In the NASA/Goddard scheme, the cloud scattering is included whereas in GFDL scheme cloud scattering is not considered explicitly. Those areas having higher absorption in NG are matching with the areas of higher amounts of clouds.

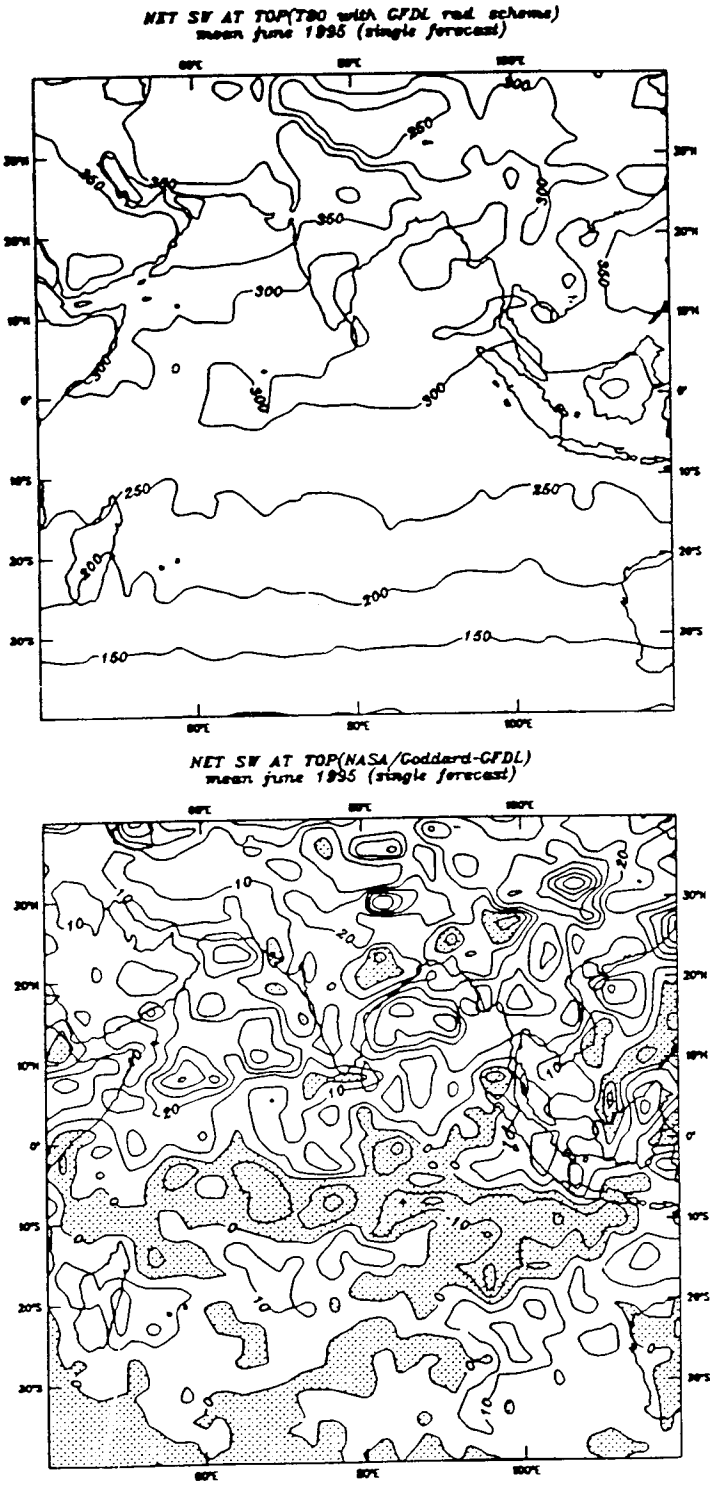

Fig. 6. Net shortwave radiation at the top of the atmosphere averaged over 30 days integration of GF (top: contour interval 50 W/m^2) and difference NG-GF (bottom: contour interval is 10 W/m^2).

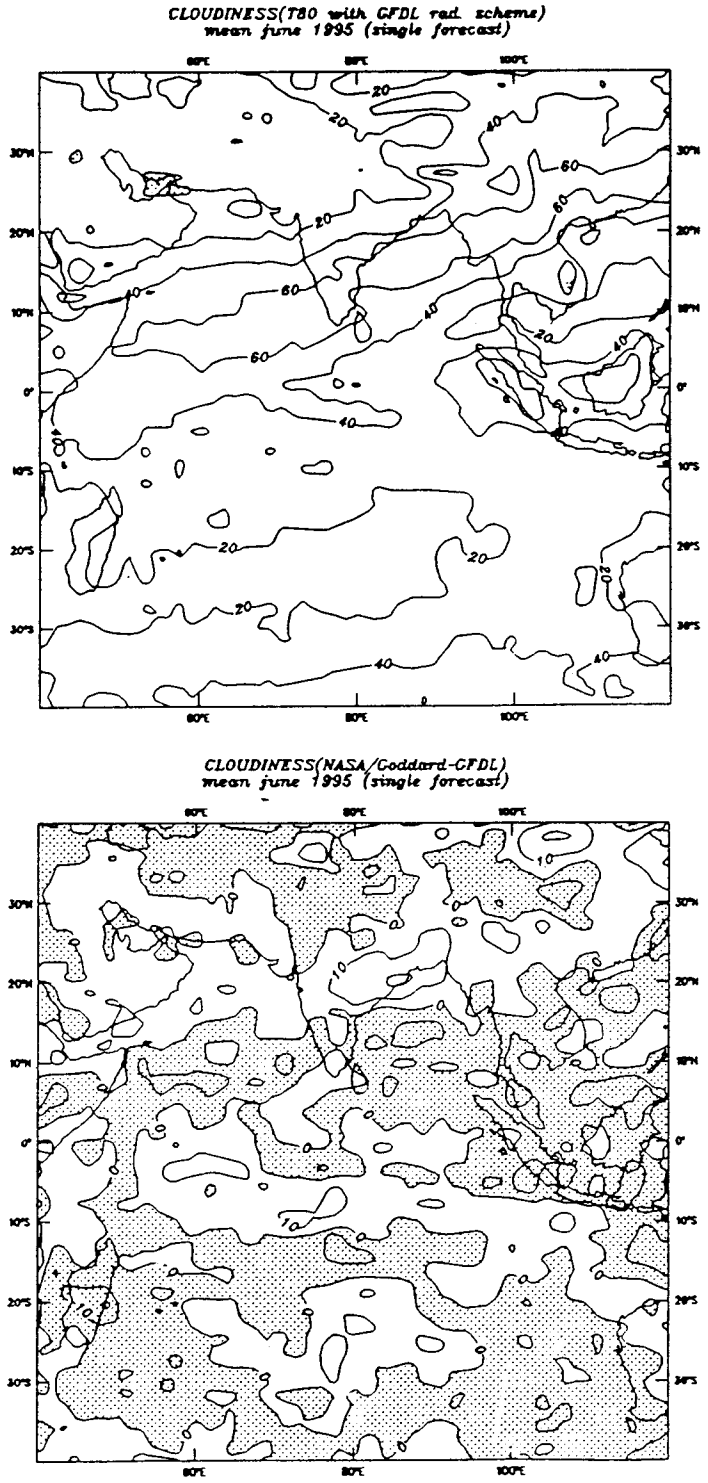

Fig. 7. As in Fig. 6, but for cloudiness. Contour intervals are 20 percent (top) and 10 percent (bottom).

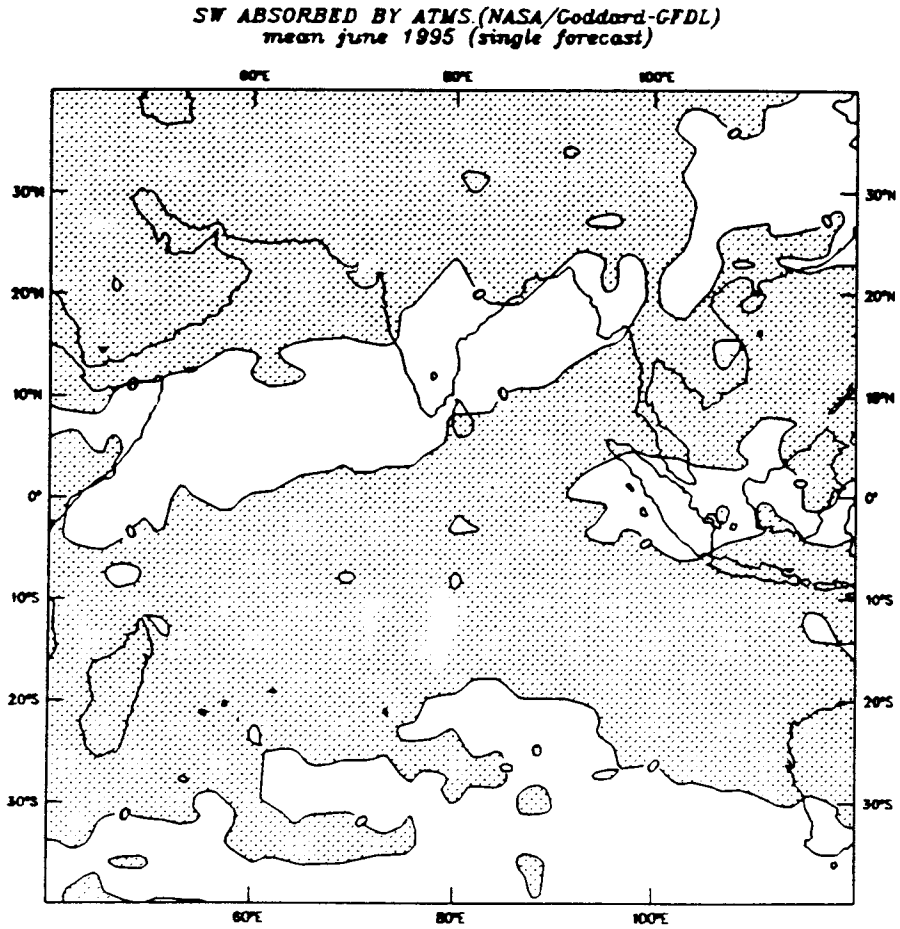

Fig. 8. Mean difference (of 30 day integration) of the shortwave flux absorbed by the atmosphere NG-GF (contour interval is 10 W/m^2).

Figure 9 shows the net shortwave radiation at the surface. Over most parts of less cloudy land regions, NG shows higher surface absorption which in turn reflected in the surface temperature (Fig. 10). It is also noticed that the 0-1°K higher surface temperature over almost all land surface areas and much higher (1-4°K) values over Himalayas where snow exists. The possible explanation of the higher surface absorption in the NG is as follows. In NG direct and diffuse radiations are treated separately and zenith angle dependent surface reflectivity is assumed. But in GF, there is no demarkation between direct and diffused radiation and hence we are using diffuse surface albedo only.

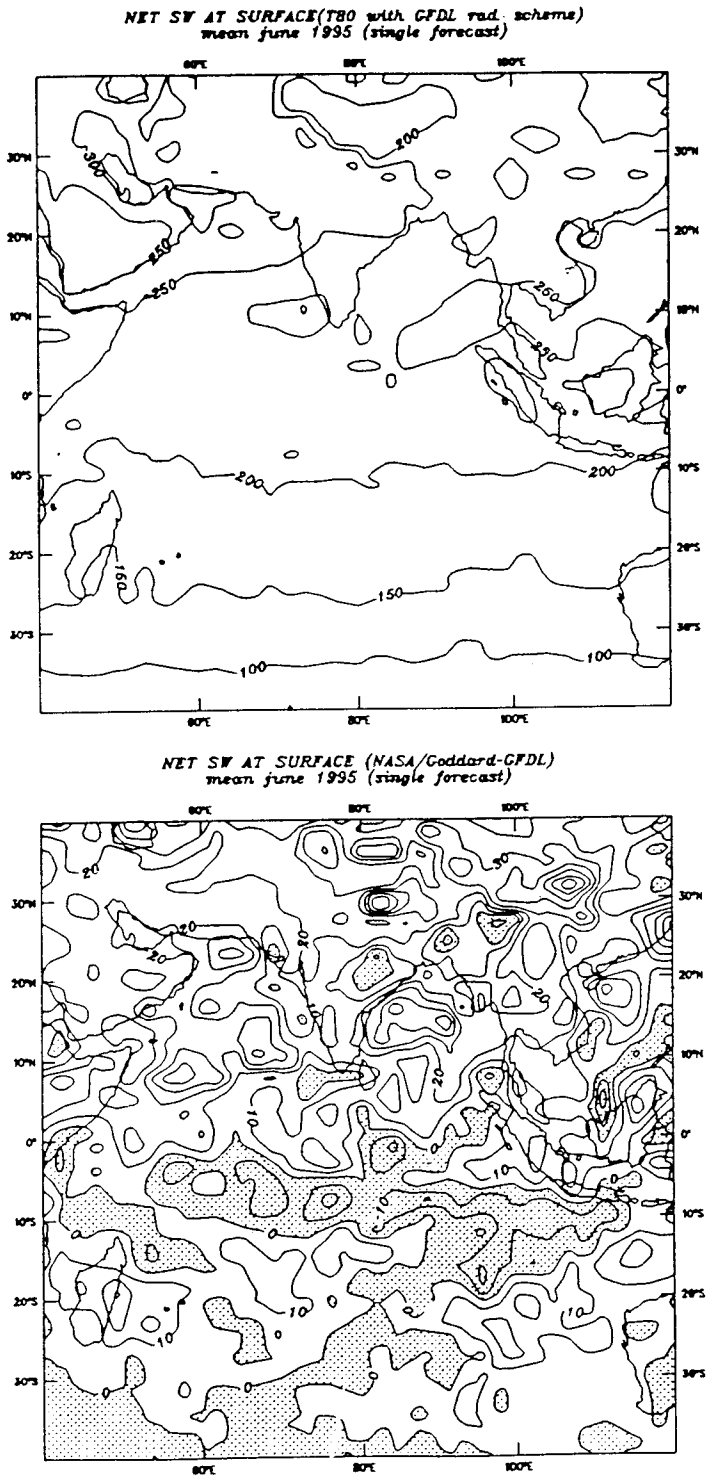

Fig. 9. As in Fig. 6, but for net shortwave at surface. Contour intervals are 50 W/m^2 (top) and 10 W/m^2 (bottom).

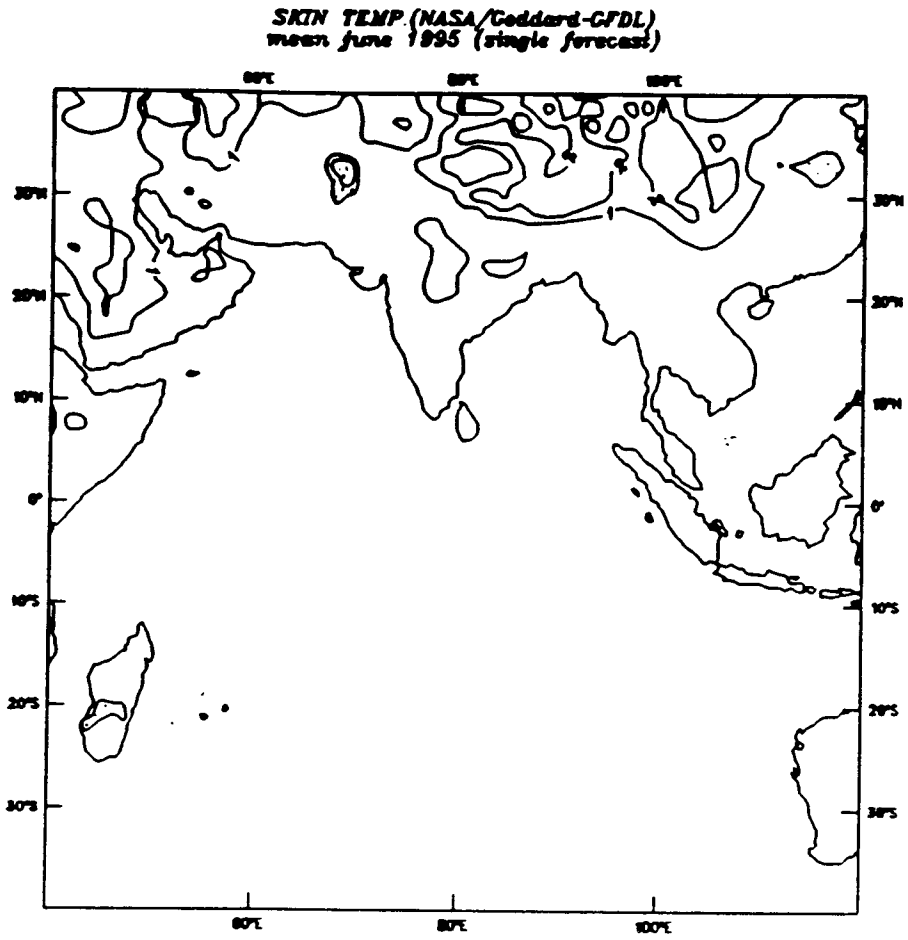

Fig. 10. As in Fig. 8, but for surface (skin) temperature. Contour interval is -4, -2, -1, 1, 2, 4° K

3.2.2 Longwave fluxes over Monsoon region

At the top of the atmosphere, the monthly mean OLR produced by both models (Fig. 11) are not very different each other and they follow the climatology. Both models are able to capture the climatological lower OLR values over peninsular India, north-east Indian and adjoining regions and over Indonesian islands. Along the south west cost of India, the OLR values are slightly smaller in NG. But over north-west part of India NG OLR values are little higher as compared to GF . Over Arabian desert and adjoining Pakistan and north west India, the OLR values are high in both the models as compared to the climatology.

Figure 12 illustrates net longwave flux reaching the surface. The difference between NG and GF is positive over those regions where cloud amounts are high (more than 20%). The differences in the cloud emissivity is an important factor in this regard.

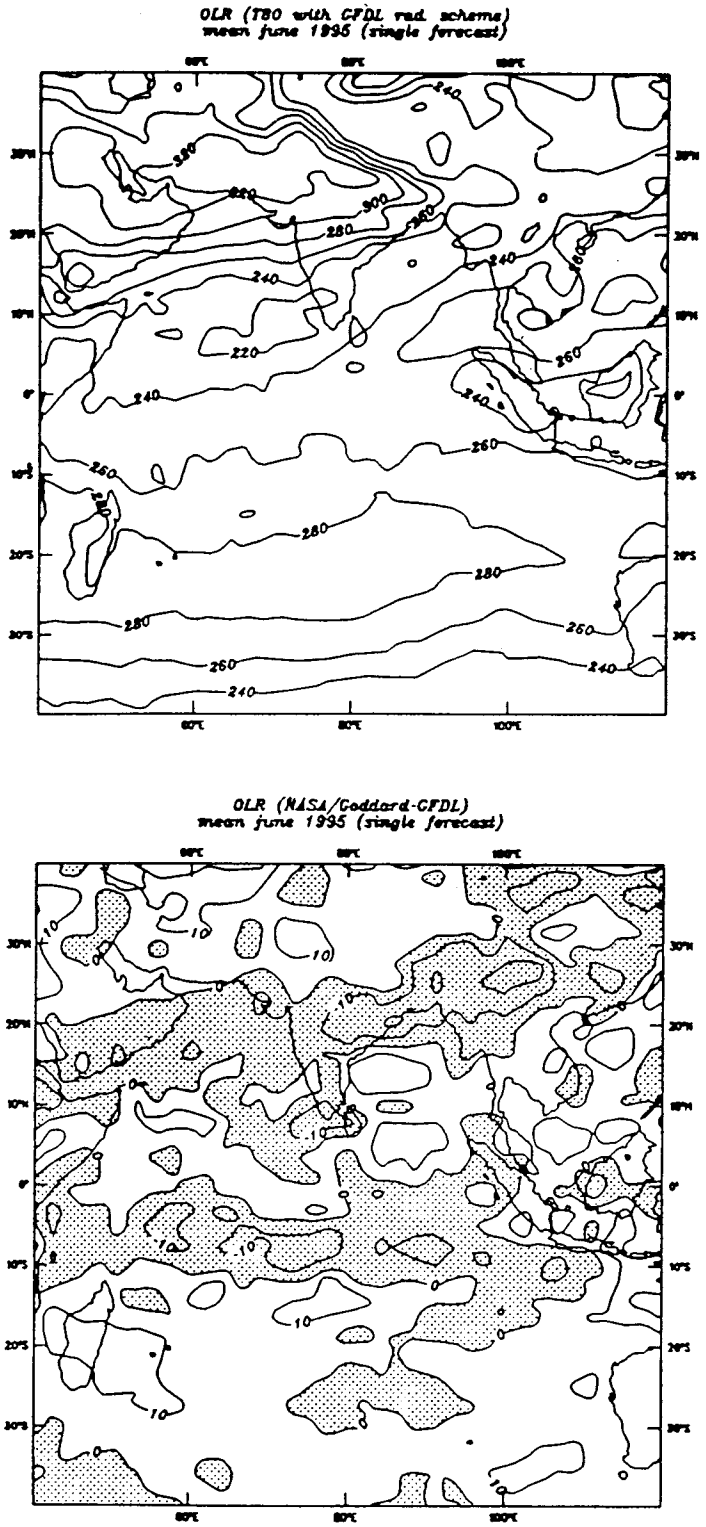

Fig. 11. As in Fig. 6, but for outgoing longwave radiation (OLR). Contour intervals are 20 W/m^2 (top) and 10 W/m^2 (bottom)

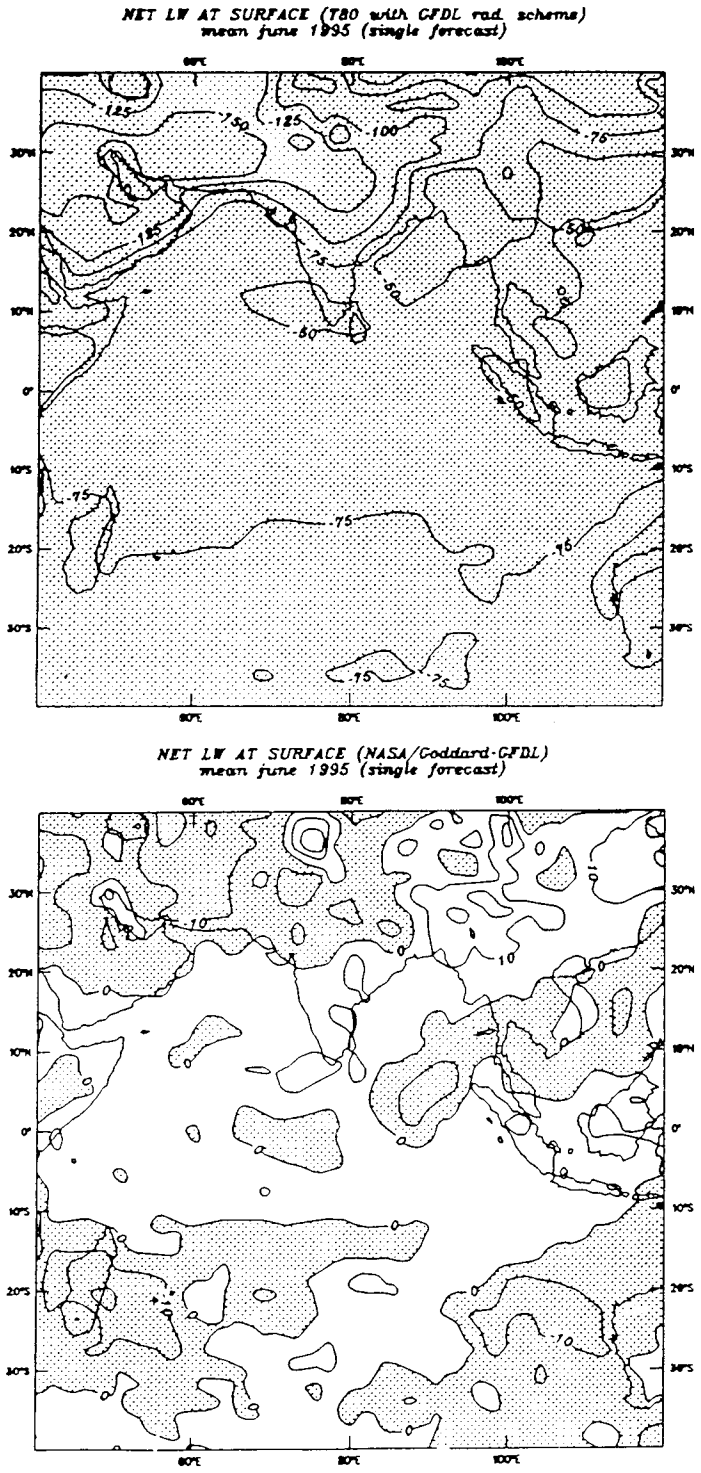

Fig. 12. As in Fig. 6, but for net longwave flux at surface. Contour intervals are 25 W/m^2 (top) and 10 W/m^2 (bottom).

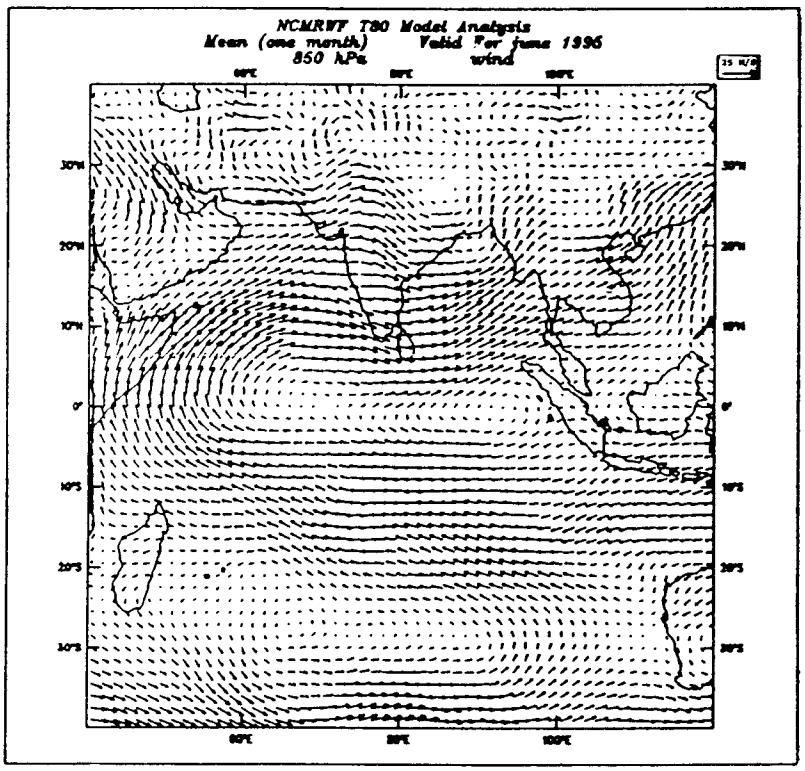

Fig. 13. Mean NCMRWF wind analysis, June 1995 (850 hPa).

3.3 Circulation features

3.3.1 Lower tropospheric features (850 hPa)

Cross equatorial flow (mainly over Somali coast), strong westerlies over the Arabian sea, peninsular India and the Bay of Bengal and the seasonal trough along the Gangetic plain are the main June climatological features directly affecting the weather over the Indian-sub continent. Mean NCMRWF June analysis shows (Fig. 13) monsoon westerlies over peninsular India having a speed of 10-15 m/s. Flow over south China is also in the range of 10-15 m/s. The analysis indicates cross equatorial flow of 15-20 m/s over African coast. Weak cross equatorial flow over east of 75°E longitude is also seen in the analysis. Seasonal trough over the Gangetic plains running from head bay to east Pakistan (heat low region) is reflected in the mean analysis of June, 1995. The centre of the subtropical high (Mascarean high) is seen over 68°E longitude and 27°S latitude in the mean analysis. The mean June 1995 flow simulated by both models show weaker cross equatorial flow over the African coast and strong monsoon westerlies over peninsular India and the Bay of Bengal (Fig. 14). The detailed comparison shows that forecast errors in the cross equatorial flow is small in NG as compared to GF (Fig. 15). Also, the position of the Mascarean high and the strength of the outflow from this anticyclone is better simulated in NG. The possible explanation for this is as follows. The higher land surface temperature leads to larger land-sea temperature contrast and hence the pressure gradient. This enhances the cross equatorial flow. But the forecast westerly errors are more over the Bay of Bengal in NG. Also, strength of the cross equatorial flow east of 75°E is more in NG. Both models produced westerly forecast errors over Bay of Bengal. But in NG, the larger land-sea temperature contrast leads to more intensification of the westerlies. The enhanced flow also increases the surface evaporation.

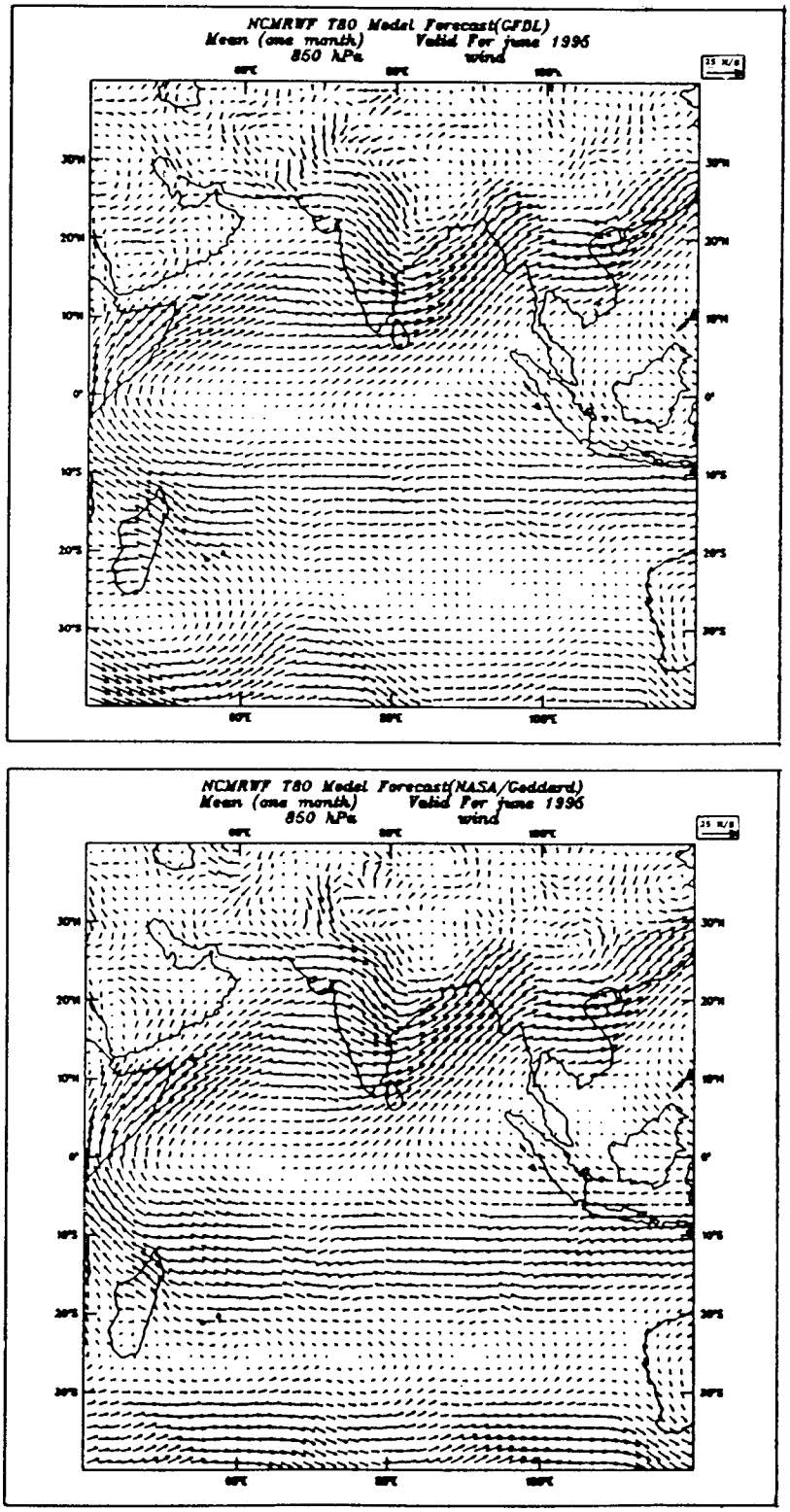

Fig. 14. Mean June simulation of wind field (850 h Pa) by GF (top) and NG (bottom).

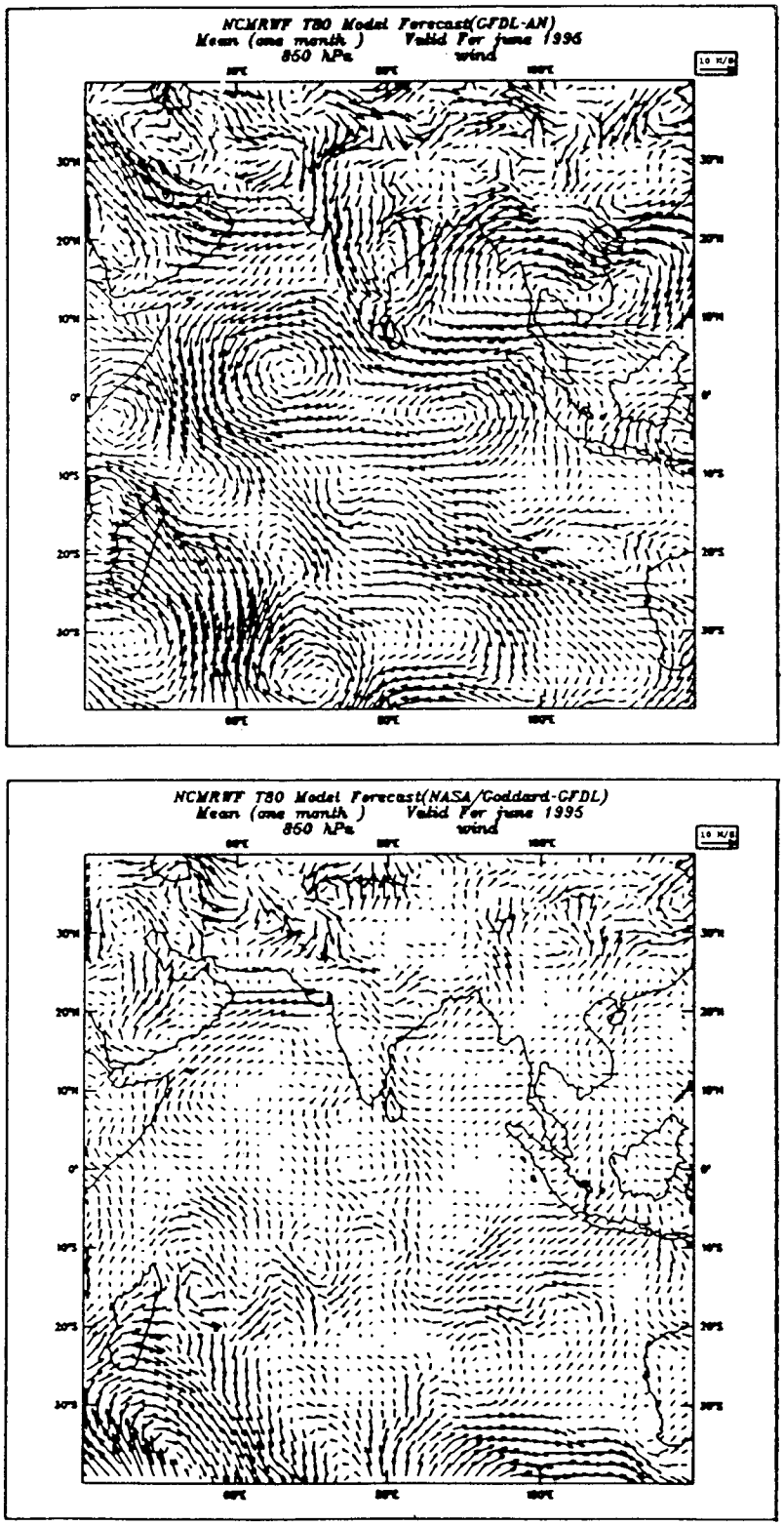

Fig. 15. Forecast errors (forecast - analysis) of GF (top) and the difference of the forecast errors of NG and GF (bottom) [850 hPa, wind].

3.3.2 Upper tropospheric features (200 hPa)

Tibetian anticyclone and strong easterlies over peninsular India are the characteristic features in the 200 hPa mean June climatology. These features are brought out in the mean analysis of June 1995 (Fig. 16) although the strength of the easterlies is less as compared to climatology. In the simulation by both models (Fig. 17), easterlies are stronger over peninsular India as compared to the analysis. The position of the Tibetian anticyclone is also different. A trough in the westerlies is present in the GF simulation which is not seen in the analysis as well as the simulation by NG. Because of this trough the anticyclone is broken into two cells in GF, one over Arabian sub continent and another over China. Single cell anticyclonic pattern is seen in the mean analysis and is simulated by NG even though the simulation slightly misplaced the centre of the anticyclone. Because of the trough along 80°E longitude is simulated by the model, which was not realized, large cyclonic forecast errors are seen (Fig. 18) over that region. Even in the NG, cyclonic forecast errors are seen over this region but is small compared to GF.

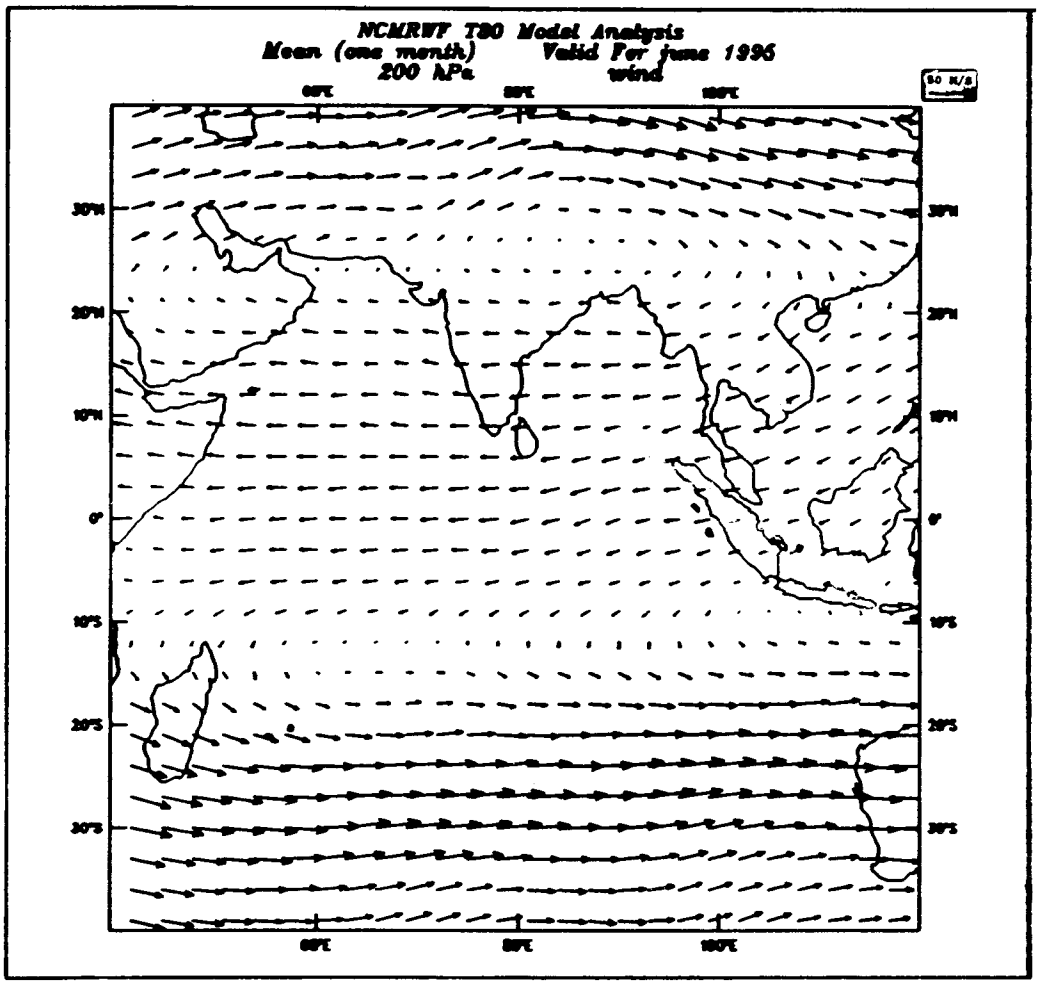

Fig. 16. Mean NCMRWF wind analysis, June 1995 (200 hPa).

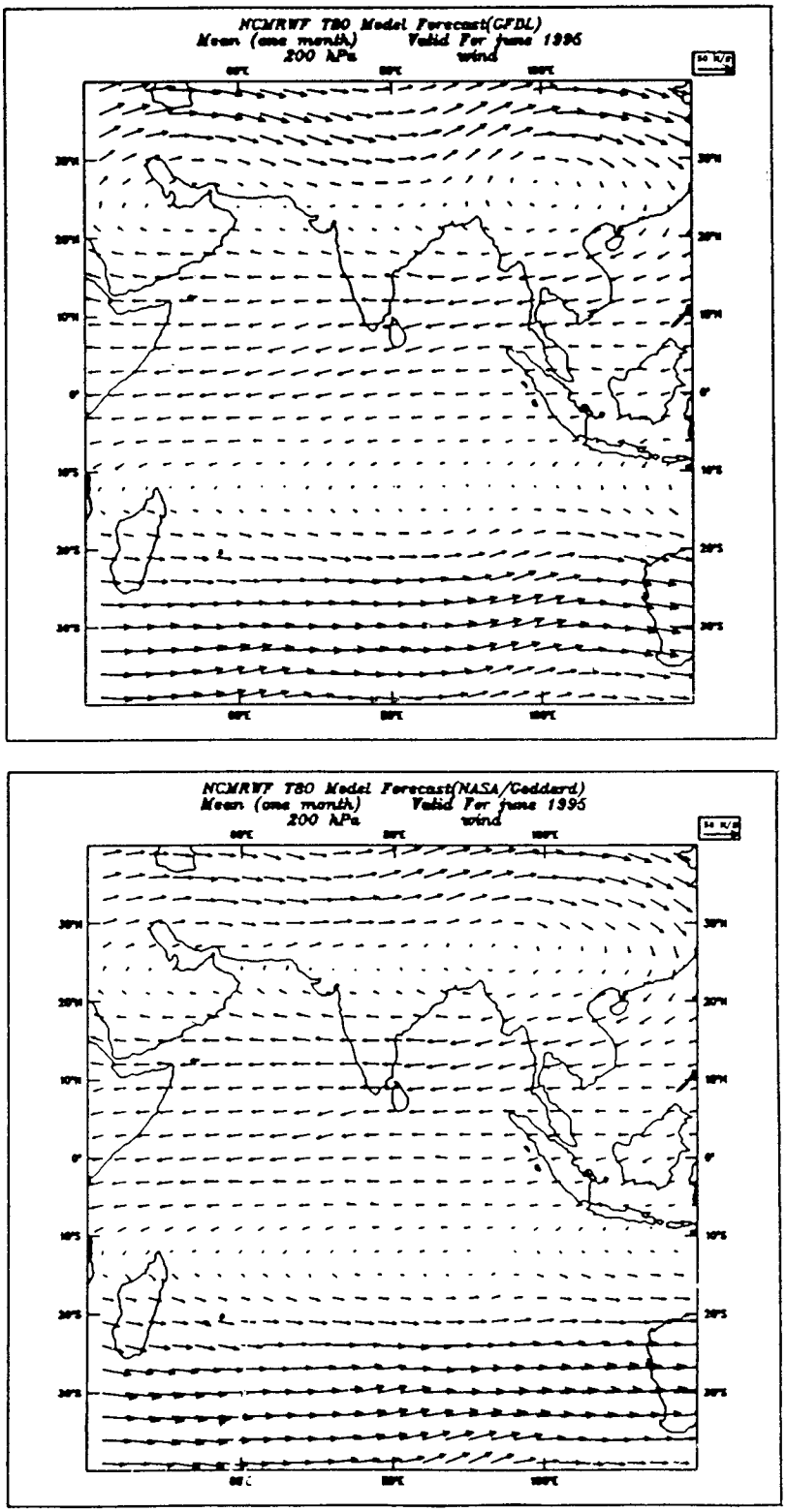

Fig. 17. Mean June simulation of wind field (200 hPa) by GF (top) and NG (bottom).

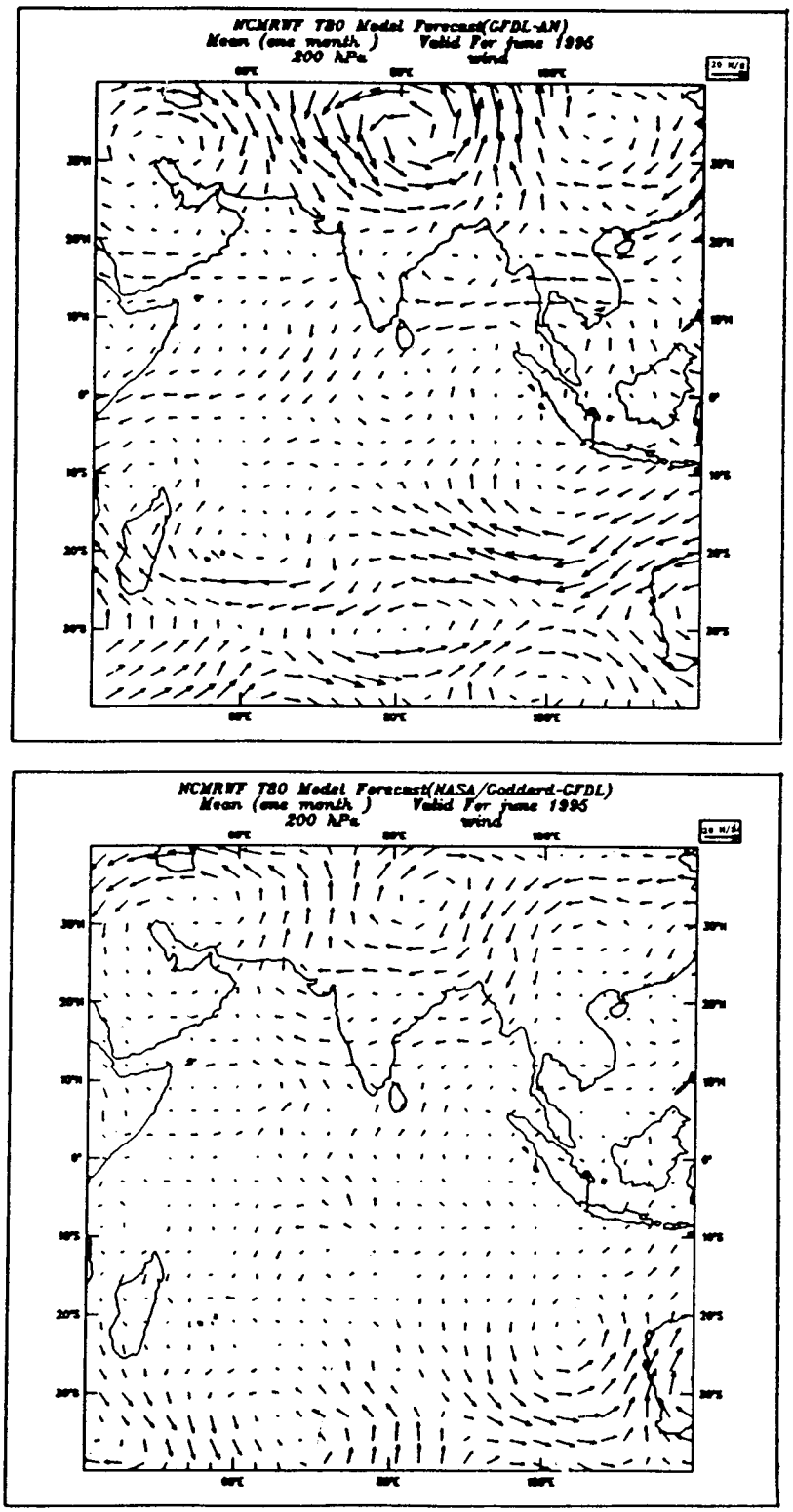

Fig. 18. Forecast errors (forecast - analysis) of GF (top) and the difference of the forecast errors of NG and GF (bottom) [200 hPa, wind].

4. Summary and Conclusions

We have computed and compared the global energy budgets of June 1995 produced by NG and GF. All mean radiation fluxes over India and the neighbourhood are also computed for June 1995. The model produced energy budgets are compared with climatological and empirical model data given by Ramanathan, 1987. These comparisons show that both models are stable and capable of producing reasonable results beyond medium range prediction. The significant difference noted between the models is the shortwave flux absorbed by the surface. NG shows higher shortwave absorption and hence higher land surface temperature. This resulted in the higher evaporation rates and higher precipitation. It is noted that, NG shows more acceptable energy balance between the incoming and outgoing fluxes (both radiational and turbulent). The mean radiative fluxes over the Indian region of NG and GF emphasises the importance of the explicit consideration of cloud scattering and better surface albedo formulations in the radiation parameterization schemes.

In addition, these models are able to produce mean circulation features for June, 1995. All important monsoon features are reproduced by both models even though some differences exist. As far as forecast errors in the flow field at lower troposphere (850 hPa) are concerned, NG has less deviation from varifying NCMRWF analysis west of 75°E, whereas GF is slightly better over the Bay of Bengal and south-east Asia. Higher net shortwave radiation at surface and hence increased surface temperature in NG as compared to GF explains the westerly forecast errors noted in NG east of 75°E longitude. In upper troposphere, the performance of NG is slightly superior over most of the regions.

Also, in general, we have find that:

(i) The influence of the changes in radiation fluxes at the surface on surface temperature prediction has more impact on the simulation of the onset phase of the monsoon as compared to the changes in the atmospheric radiative heating/cooling rates.

(ii) Differences in the forecast errors of GFDL radiation scheme and NASA/Goddard radiation scheme in T80 model in the lower and upper troposphere reveal the importance of a good radiation scheme in medium and extended range prediction. Thus, models with reasonably good physical process parameterization schemes including radiation may be able to produce realistic mean monthly monsoon features.

Acknowledgement

The authors are grateful to Professor Harshvardhan, Purdue University, USA, for providing the one-dimensional NASA/Goddard radiation parameterization code. We would like to thank Dr. S. K. Mishra, Director, NCMRWF and Dr. B. K. Basu, Head, Research division, NCMRWF for extending the facilities for this work. Thanks are also due to Professor Z. H. Khan, Dept. of physics, Jamia Millia Islamia University, India, for valuable suggestions.

REFERENCES

Campana, K. A, B. K Basu and M. D Schwarzkopf, 1988. Radiative processes. NMC MRF Model documentation, 68-113.

Fels, S. B. and M. D. Schwarzkopf, 1975. The simplified exchange approximation- A new method for radiative transfer calculations. *J. Atmos. Sci.*, **32**, 1475-1488.

Harshvardhan, R. Davies, D. A. Randall and T. G. Corsetti, 1987. A fast radiation parameterization for general circulation models. *J. Geophys. Res.*, **92**, 1009-1016.

Lacis, A. A and J. E. Hansen, 1974. A parameterization for the absorption of solar radiation in the Earth's atmosphere. *J. Atmos. Sci.*, **31**, 118-133.

Morcrette, J. J, 1990. Impact of changes to radiation transfer parameterization plus cloud optical properties in the ECMWF model, *Mon. Wea. Rev.*, **118**, 847-873.

Ramanathan, V., 1987. The role of earth radiation budget studies in climate and general circulation research. *J. Geophys. Res.*, **92**, 4075-4095.

Schwarzkopf, M. D. and S. B. Fels, 1991. The simplified exchange method revisited: An accurate rapid method for computation of infrared cooling rates and fluxes. *J. Geophys. Res.*, **96**, 9075-9096.

Slingo, J. M., 1987. The development and verification of a cloud prediction scheme for the ECMWF model. *Q. J. R. Meteorol. Soc.*, **113**, 899-927.

Slingo, J. M., U. C. Mohanty, M. Tiedtke and R. P. Pearce, 1988. Prediction of 1979 summer monsoon onset with modified parameterization schemes. *Mon. Wea. Rev.*, **116**, 328-346.